

## Poly(propyleneimine) Dendrimers Peripherally Modified with Mesogens

Koichiro Yonetake\* and Toru Masuko

*Department of Materials Science and Engineering, Faculty of Engineering, Yamagata University, Yonezawa, Yamagata 992-8510, Japan*

Takashi Morishita, Kazuhiro Suzuki, and Mitsuru Ueda\*,†

*Department of Human Sensing and Functional Sensor Engineering, Graduate School of Engineering, Yamagata University, Yonezawa, Yamagata 992-8510, Japan*

Ritsuko Nagahata

*Department of Polymer Chemistry, National Institute of Materials and Chemical Research, 1-1 Higashi, Tsukuba, Ibaraki 305, Japan**Received January 26, 1999; Revised Manuscript Received June 7, 1999*

**ABSTRACT:** Poly(propyleneimine)-based liquid crystalline dendrimers (**PPILCDs**) with a relatively flexible dendritic scaffold were successfully prepared by the Michael addition reaction of poly(propyleneimine)s with  $\omega$ -(4'-cyanobiphenyloxy)alkyl acrylate (**1**). The structures of **PPILCDs** were characterized by IR spectroscopy,  $^1\text{H}$  NMR spectroscopy, and MALDI-TOF mass spectroscopy. **PPILCDs** exhibit smectic liquid crystalline natures between  $-7$  and  $+89$  °C. The temperature range of the smectic phases expanded with increases in the generation of the dendritic core and the length of flexible spacers. The homeotropic orientation was allowed to take place in **PPILCD** with the second-generation scaffold, when it was slowly cooled.

## Introduction

Dendrimers are well-defined, highly branched, and three-dimensional polymers.<sup>1,2,3</sup> Moreover, the large number of reactive end groups existing at the periphery of dendrimers easily react with many reagents to give dendrimers with various functionalities at the periphery. Therefore, they are receiving interest as new polymeric materials, such as catalysts, antennas for photoinduced energy, chiral recognition, and enantiomer separation, molecular electronics, and unimolecular micelles.<sup>4–8</sup>

The structure and properties of liquid crystalline dendrimers (LCDs) are very interesting areas of research because dendrimers are already showing promise as exciting well-defined building blocks in the production of liquid crystals. A dendrimer prepared by the convergent synthesis of the racemic AB<sub>2</sub> rodlike mesogenic dendrons was reported to display thermotropic nematic and smectic liquid crystalline phases.<sup>9</sup> Shibaev<sup>10</sup> and Frey<sup>11</sup> independently reported carbosilane-based liquid crystalline dendrimers by introducing mesogenic units as end groups. These materials were shown to display smectic mesophases. They also pointed out that the low viscosity as well as the relatively low phase transition temperature can be attributed to the dendritic topology, and the dendritic liquid crystalline polymers appear to be promising materials for optical switching and electrooptical applications. Furthermore, a dendritic aliphatic polyester functionalized with a ferroelectric mesogen has been reported to show a ferroelectric smectic C\*.<sup>12</sup> Recently, we have initiated a program to clear the structure and properties of peripherally substituted liquid crystalline

dendrimers (PSLCDs). In previous articles, we reported a synthesis and characterization of poly(amidoamine)-<sup>13</sup> and poly(propyleneimine)-based LCDs.<sup>14</sup> The former PSLCDs showed a lyotropic liquid crystallinity in 80 wt % solutions in DMF containing lithium chloride due to a relatively rigid dendritic scaffold and an amide linkage between dendrimers and mesogens. The amide bond strongly influences the rigidity of dendrimers through a strong intermolecular hydrogen bonding. The latter dendrimers composed of a relatively flexible dendritic scaffold also did not show a thermotropic liquid crystalline nature but exhibited the liquid crystalline textures in the sample sheared at 70 °C because the relatively flexible dendritic scaffold improved the mobility of the terminal mesogens compared to the former dendrimers.

The next target was to verify the properties of PSLCDs derived from poly(propyleneimine) dendrimers coupled with rigid mesogens by ester linkages. The present paper describes the synthesis and properties of poly(propyleneimine) dendrimers with mesogenic units on the surface.

## Experimental Section

**Materials.** *N*-Methyl-2-pyrrolidinone (NMP) was stirred over powdered calcium hydride overnight, distilled under reduced pressure, and then stored over 4-Å molecular sieves. Tetrahydrofuran (THF) and triethylamine (TEA) were purified by distillation. Poly(propyleneimine) dendrimers (PPIDs) were purchased from Aldrich. Other reagents and solvents were obtained commercially and used as received.

**10-Bromodecane-1-ol.** Into a 25 mL, three-neck round-bottom flask equipped with a stirrer, Dean–Stark trap, and a condenser were placed decane-1,10-diol (5.2 g, 0.03 mmol), hydrobromic acid (48% aqueous solution), and toluene (30 mL). The mixture was heated at reflux for 5 h. The solvent was evaporated to give a colorless liquid. The yield was 6.90 g (97%). IR (KBr):  $\nu$  3340 (OH), 2930  $\text{cm}^{-1}$  (CH).  $^1\text{H}$  NMR ( $\text{CDCl}_3$ ):  $\delta$  1.3–1.8 (m, 16H,  $\text{CH}_2$ ), 3.4 (t, 2H,  $\text{BrCH}_2$ ), and 3.6 (t, 2H,  $\text{HOCH}_2$ ).

\* To whom the correspondence should be addressed.

† Telephone and Fax: +81 3 5734 2127. E-mail: mueda@polymer.titech.ac.jp.

**4'-(10-Hydroxydecyloxy)-4-biphenylcarbonitrile.** A mixture of 4'-hydroxy-4-biphenylcarbonitrile (6.26 g, 0.024 mol) and KOH (1.55 g, 0.024 mol) in ethanol (30 mL) was refluxed for 20 min. To this solution was added dropwise a solution of 10-bromodecane-1-ol (6.26 g, 0.026 mol) in ethanol (5 mL) at room temperature. After addition, the reaction mixture was refluxed for 24 h, and the solvent was evaporated. The residue was extracted with diethyl ether, and the ether layer was washed with aqueous saturated sodium carbonate solution and dried over anhydrous magnesium sulfate. The solvent was evaporated to produce a white solid. Recrystallization from methanol gave white needles, mp 138–139 °C. The yield was 5.90 g (70%). IR (KBr):  $\nu$  3290 (OH), 2920 (CH), and 2230  $\text{cm}^{-1}$  (CN).  $^1\text{H}$  NMR ( $\text{CDCl}_3$ ):  $\delta$  1.3–1.8 (m, 16H,  $\text{CH}_2$ ), 3.6 (t, 2H,  $\text{HOCH}_2$ ), 4.0 (t, 2H,  $\text{PhOCH}_2$ ), and 6.9–7.6 ppm (m, 8H, ArH). Anal. Calcd for  $\text{C}_{23}\text{H}_{29}\text{NO}_2$ : C, 78.59; H, 8.31; N, 3.98. Found: C, 78.24; H, 8.26; N, 3.91.

**4'-(6-Hydroxyhexyloxy)-4-biphenylcarbonitrile.** This compound was prepared from 6-bromohexane-1-ol and 4'-hydroxy-4-biphenylcarbonitrile as described above. Recrystallization from methanol/water gave white needles, mp 94–96 °C. The yield was 47%. IR (KBr):  $\nu$  3330 (OH), 2940, 2870 (CH), and 2230  $\text{cm}^{-1}$  (CN).  $^1\text{H}$  NMR ( $\text{CDCl}_3$ ):  $\delta$  1.4–1.8 (m, 8H,  $\text{CH}_2$ ), 3.6 (t, 2H,  $\text{HOCH}_2$ ), 4.0 (t, 2H,  $\text{PhOCH}_2$ ), and 7.0–7.7 ppm (m, 8H, ArH). Anal. Calcd for  $\text{C}_{19}\text{H}_{21}\text{NO}_2$ : C, 77.26; H, 7.16; N, 4.74. Found: C, 77.20; H, 7.34; N, 4.63.

**4'-(8-Hydroxyoctyloxy)-4-biphenylcarbonitrile.** This compound was prepared from 8-bromohexane-1-ol and 4'-hydroxy-4-biphenylcarbonitrile as described above. Recrystallization from methanol/water gave white needles, mp 92–94 °C. The yield was 39%. IR (KBr):  $\nu$  3330 (OH), 2940, 2860 (CH), and 2220  $\text{cm}^{-1}$  (CN).  $^1\text{H}$  NMR ( $\text{CDCl}_3$ ):  $\delta$  1.4–1.9 (m, 10H,  $\text{CH}_2$ ), 3.6 (t, 2H,  $\text{HOCH}_2$ ), 4.0 (t, 2H,  $\text{PhOCH}_2$ ), and 7.0–7.7 ppm (m, 8H, ArH). Anal. Calcd for  $\text{C}_{21}\text{H}_{25}\text{NO}_2$ : C, 77.98; H, 7.79; N, 4.33. Found: C, 77.94; H, 7.96; N, 4.25.

**10-(4'-Cyanobiphenyloxy)decyl acrylate (1-C-10).** A solution of acryloyl chloride (0.475 mL, 5.85 mmol) was added dropwise to an ice-cooled solution of 4'-(10-hydroxydecyloxy)-4-biphenyl carbonitrile (1.58 g, 4.5 mmol) and TEA (0.62 mL) in THF (9 mL). After addition, the mixture was stirred for 12 h at room temperature, and the solvent was evaporated. The residue was extracted with diethyl ether, and the ether layer was washed with water and dried over anhydrous magnesium sulfate. The solvent was evaporated under pressure to produce a white solid. Recrystallization from methanol gave white needles, mp 73–75 °C. The yield was 1.22 g (67%). IR (KBr):  $\nu$  2910 and 2850 (CH), 2220 (CN), 1720  $\text{cm}^{-1}$  (COOR).  $^1\text{H}$  NMR ( $\text{CDCl}_3$ ):  $\delta$  1.3 (m, 12H,  $\text{CH}_2$ ), 1.6 (m, 2H,  $\text{CH}_2$ ), 1.6 (m, 2H,  $\text{CH}_2$ ), 4.0 (t, 2H,  $\text{PhOCH}_2$ ), 4.1 (t, 2H,  $\text{COOCH}_2$ ), 5.8 (dd, 1H,  $\text{CH}=\text{CH}$ ), 6.12 (dd, 1H,  $\text{CH}_2=\text{CH}$ ), 6.4 (dd, 1H,  $\text{CH}=\text{CH}$ ), 7.0 (d, 2H, ArH), 7.5 (d, 2H, ArH), 7.6 (d, 2H, ArH), and 7.7 ppm (d, 2H, ArH). Anal. Calcd for  $\text{C}_{26}\text{H}_{31}\text{NO}_3$ : C, 77.0; H, 7.70; N, 3.45. Found: C, 77.17; H, 7.73; N, 3.38.

**6-(4'-Cyanobiphenyloxy)hexyl Acrylate (1-C-6).** This compound was prepared from 4'-(6-hydroxyhexyloxy)-4-biphenylcarbonitrile and acryloyl chloride as described above. Recrystallization from methanol gave white needles, mp 76–78 °C. The yield was 71%. IR (KBr):  $\nu$  2940 and 2860 (CH), 2220 (CN), 1720  $\text{cm}^{-1}$  (COOR).  $^1\text{H}$  NMR ( $\text{CDCl}_3$ ):  $\delta$  1.3 (m, 4H,  $\text{CH}_2$ ), 1.6 (m, 2H,  $\text{CH}_2$ ), 1.6 (m, 2H,  $\text{CH}_2$ ), 4.0 (t, 2H,  $\text{PhOCH}_2$ ), 4.2 (t, 2H,  $\text{COOCH}_2$ ), 5.8 (dd, 1H,  $\text{CH}=\text{CH}$ ), 6.13 (dd, 1H,  $\text{CH}_2=\text{CH}$ ), 6.4 (dd, 1H,  $\text{CH}=\text{CH}$ ), 7.0 (d, 2H, ArH), 7.5 (d, 2H, ArH), 7.6 (d, 2H, ArH), and 7.7 ppm (d, 2H, ArH). Anal. Calcd for  $\text{C}_{22}\text{H}_{23}\text{NO}_3$ : C, 75.62; H, 6.63; N, 4.01. Found: C, 75.88; H, 6.86; N, 3.98.

**8-(4'-Cyanobiphenyloxy)octyl Acrylate (1-C-8).** Recrystallization from methanol gave white needles, mp 77–79 °C. The yield was 79%. IR (KBr):  $\nu$  2950 and 2870 (CH), 2220 (CN), 1720  $\text{cm}^{-1}$  (COOR).  $^1\text{H}$  NMR ( $\text{CDCl}_3$ ):  $\delta$  1.3 (m, 6H,  $\text{CH}_2$ ), 1.6 (m, 2H,  $\text{CH}_2$ ), 1.6 (m, 2H,  $\text{CH}_2$ ), 4.0 (t, 2H,  $\text{PhOCH}_2$ ), 4.2 (t, 2H,  $\text{COOCH}_2$ ), 5.8 (dd, 1H,  $\text{CH}=\text{CH}$ ), 6.12 (dd, 1H,  $\text{CH}_2=\text{CH}$ ), 6.4 (dd, 1H,  $\text{CH}=\text{CH}$ ), 7.0 (d, 2H, ArH), 7.5 (d, 2H, ArH), 7.6 (d, 2H, ArH), and 7.7 ppm (d, 2H, ArH). Anal. Calcd for  $\text{C}_{24}\text{H}_{27}\text{NO}_3$ : C, 76.36; H, 7.21; N, 3.71. Found: C, 76.52; H, 7.47; N, 3.66.

**The First-Generation-Poly(propyleneimine) Liquid Crystalline Dendrimer (PPILCD-1-C-10).** A solution of poly(propyleneimine) dendrimer (0.063 g, 0.2 mmol) and mesogen (1-C-10) (0.742 g, 2.4 mmol) in THF (2 mL) was stirred at 50 °C for 1 week. After evaporation of the solvent, the product was purified by extraction with ethanol several times at 70 °C to remove excess mesogens. The yield was 0.56 g (79%). IR (KBr):  $\nu$  2230 (CN), 1730  $\text{cm}^{-1}$  (COOR).  $^1\text{H}$  NMR ( $\text{CDCl}_3$ ):  $\delta$  1.55 (m, 140 H,  $\text{CH}_2$ ), 2.43 (m, 36H,  $\text{CH}_2$ ), 2.76 (t, 16H,  $\text{CH}_2$ ), 3.99 (t, 16H,  $\text{CH}_2$ ), 4.03 (t, 16H,  $\text{CH}_2$ ), 6.97 (d, 16H, ArH), 7.51 (d, 16H, ArH), 7.62 (d, 16H, ArH), and 7.67 ppm (d, 16H, ArH). Anal. Calcd for  $\text{C}_{224}\text{H}_{288}\text{N}_{14}\text{O}_{24}$ : C, 66.22; H, 5.96; N, 11.19. Found: C, 66.42; H, 5.73; N, 11.18. MALDI-TOF MS: molecular weight calculated for  $\text{C}_{224}\text{H}_{288}\text{N}_{14}\text{O}_{24}$ ,  $m/z$  = 3561.8.  $[\text{M} + \text{H}]^+$ ; found,  $m/z$  = 3563.3  $[\text{M} + \text{H}]^+$ ;  $M_w/M_n$  = 1.05.

**The First-Generation-Poly(propyleneimine) Liquid Crystalline Dendrimer PPILCD-1-C-8.** This compound was prepared from PPID-1 and mesogen 1-C-8 as described above. The yield was 59%. IR (KBr):  $\nu$  2220 (CN), 1720  $\text{cm}^{-1}$  (COOR).  $^1\text{H}$  NMR ( $\text{CDCl}_3$ ):  $\delta$  1.55 (m, 108 H,  $\text{CH}_2$ ), 2.43 (m, 36H,  $\text{CH}_2$ ), 2.77 (t, 16H,  $\text{CH}_2$ ), 3.98 (t, 16H,  $\text{CH}_2$ ), 4.04 (t, 16H,  $\text{CH}_2$ ), 6.97 (d, 16H, ArH), 7.51 (d, 16H, ArH), 7.62 (d, 16H, ArH), 7.68 ppm (d, 16H, ArH). Molecular weight calculated for  $\text{C}_{208}\text{H}_{256}\text{N}_{14}\text{O}_{24}$ :  $m/z$  = 3359.4,  $[\text{M} + \text{Na}]^+$ . Found:  $m/z$  = 3359.0,  $[\text{M} + \text{Na}]^+$ .  $M_w/M_n$  = 1.06.

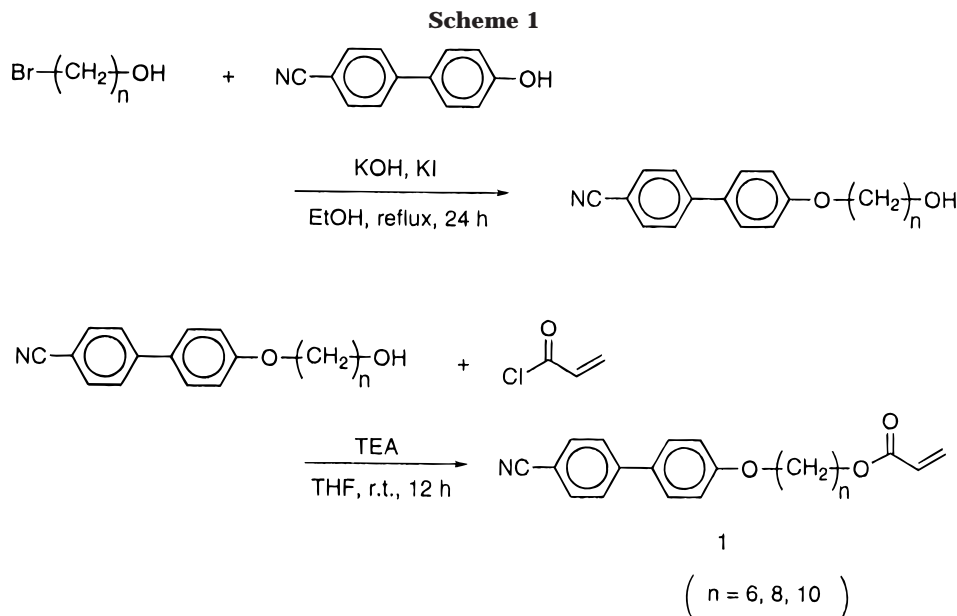
**The First-Generation-Poly(propyleneimine) Liquid Crystalline Dendrimer PPILCD-1-C-6.** This compound was prepared from PPID-1 and mesogen 1-C-6 as described above. The yield was 40%. IR (KBr):  $\nu$  2220 (CN), 1720  $\text{cm}^{-1}$  (COOR).  $^1\text{H}$  NMR ( $\text{CDCl}_3$ ):  $\delta$  1.55 (m, 76 H,  $\text{CH}_2$ ), 2.43 (m, 36H,  $\text{CH}_2$ ), 2.76 (t, 16H,  $\text{CH}_2$ ), 3.98 (t, 16H,  $\text{CH}_2$ ), 4.08 (t, 16H,  $\text{CH}_2$ ), 6.96 (d, 16H, ArH), 7.51 (d, 16H, ArH), 7.61 (d, 16H, ArH), and 7.67 ppm (d, 16H, ArH). Molecular weight calculated for  $\text{C}_{192}\text{H}_{224}\text{N}_{14}\text{O}_{24}$ :  $m/z$  = 3135.0,  $[\text{M} + \text{Na}]^+$ . Found:  $m/z$  = 3134.2,  $[\text{M} + \text{Na}]^+$ .  $M_w/M_n$  = 1.05.

**The Second-Generation-Poly(propyleneimine) Liquid Crystalline Dendrimer PPILCD-2-C-10.** This compound was prepared from PPID-2 and mesogen 1-C-10 as described above. The yield was 0.75 g (52%). IR (KBr):  $\nu$  2230 (CN), 1730  $\text{cm}^{-1}$  (COOR).  $^1\text{H}$  NMR ( $\text{CDCl}_3$ ):  $\delta$  1.55 (m, 284H,  $\text{CH}_2$ ), 2.42 (m, 84H,  $\text{CH}_2$ ), 2.76 (t, 32H,  $\text{CH}_2$ ), 3.97 (t, 32H,  $\text{CH}_2$ ), 4.03 (t, 32H,  $\text{CH}_2$ ), 6.97 (d, 32H, ArH), 7.51 (d, 32H, ArH), 7.62 (d, 32H, ArH), and 7.67 ppm (d, 32H, ArH). Anal. Calcd for  $\text{C}_{456}\text{H}_{592}\text{N}_{30}\text{O}_{48}$ : C, 66.22; H, 5.96; N, 11.19. Found: C, 66.42; H, 5.73; N, 11.18. MALDI-TOF MS: molecular weight calculated for  $\text{C}_{456}\text{H}_{592}\text{N}_{30}\text{O}_{48}$ ,  $m/z$  = 7263.0,  $[\text{M} + \text{H}]^+$ ; found,  $m/z$  = 7268.5,  $[\text{M} + \text{H}]^+$ ;  $M_w/M_n$  = 1.09.

**The Second-Generation-Poly(propyleneimine) Liquid Crystalline Dendrimer PPILCD-2-C-8.** The yield was 79%. This compound was prepared from PPID-2 and mesogen 1-C-8 as described above. IR (KBr):  $\nu$  2220 (CN), 1730  $\text{cm}^{-1}$  (COOR).  $^1\text{H}$  NMR ( $\text{CDCl}_3$ ):  $\delta$  1.55 (m, 220 H,  $\text{CH}_2$ ), 2.43 (m, 84H,  $\text{CH}_2$ ), 2.76 (t, 32H,  $\text{CH}_2$ ), 3.96 (t, 32H,  $\text{CH}_2$ ), 4.03 (t, 32H,  $\text{CH}_2$ ), 6.96 (d, 32H, ArH), 7.50 (d, 32H, ArH), 7.61 (d, 32H, ArH), 7.66 ppm (d, 32H, ArH). Molecular weight calculated for  $\text{C}_{424}\text{H}_{496}\text{N}_{30}\text{O}_{48}$ :  $m/z$  = 6803.8,  $[\text{M} + \text{Na}]^+$ . Found:  $m/z$  = 6803.6,  $M_w/M_n$  = 1.07.

**The Second-Generation-Poly(propyleneimine) Liquid Crystalline Dendrimer PPILCD-2-C-6.** The yield was 87%. This compound was prepared from PPID-2 and mesogen 1-C-6 as described above. IR (KBr):  $\nu$  2220 (CN), 1730  $\text{cm}^{-1}$  (COOR).  $^1\text{H}$  NMR ( $\text{CDCl}_3$ ):  $\delta$  1.55 (m, 156 H,  $\text{CH}_2$ ), 2.45 (m, 84H,  $\text{CH}_2$ ), 2.76 (t, 32H,  $\text{CH}_2$ ), 3.96 (t, 32H,  $\text{CH}_2$ ), 4.06 (t, 32H,  $\text{CH}_2$ ), 6.94 (d, 32H, ArH), 7.49 (d, 32H, ArH), 7.59 (d, 32H, ArH), 7.65 ppm (d, 32H, ArH). Molecular weight calculated for  $\text{C}_{392}\text{H}_{464}\text{N}_{30}\text{O}_{48}$ :  $m/z$  = 6387.2,  $[\text{M} + \text{Na}]^+$ . Found:  $m/z$  = 6389.4,  $[\text{M} + \text{Na}]^+$ .  $M_w/M_n$  = 1.06.

**Measurements.** FT-IR spectra were measured on a Horiba FT-210 spectrophotometer.  $^1\text{H}$  NMR spectra were recorded on a JEOL EX 270 spectrometer. Thermal analyses were performed on a Seiko SSS 5000 TG-DTA 220 thermal analyzer at a heating rate of 10 °C/min for thermogravimetry (TG) and a Seiko SSS5000 DSC 220 at a heating rate of 10 °C/min for differential scanning calorimetry (DSC) under nitrogen. Mo-



molecular weights were determined by a gel permeation chromatograph (GPC) with polystyrene calibration using a JASCO HPLC equipped with Shodex KF-80 M column at 40 °C in THF. MALDI-TOF spectra were obtained by a KRATOS KOMPACT MALDI III mass spectrometer (SHIMADZU CORPORATION, Kyoto, Japan) operated in the linear-positive mode. This instrument uses a 337 nm nitrogen laser with a 3 ns pulse duration for ionization and an electron multiplier detector. The samples were dissolved in tetrahydrofuran and mixed with sinapinic acid or 2,5-dihydroxybenzoic acid as the matrix. Optical textures of the samples were examined using the polarizing optical microscope (POM) equipped with a hot stage (Linkam Co., TH-600RMS) under nitrogen. X-ray diffraction experiments were carried out on a RAD-ra diffractometer (Rigaku Denki Co. Ltd.) equipped with a heating device. Nickel-filtered Cu K $\alpha$  radiation was employed. Wide-angle X-ray scattering (WAXS) traces were recorded by a scintillation counter system with a 1.0 mm diameter pinhole collimator and 1  $\times$  1° receiving slit. The diffractometry was performed in transmission. The WAXS traces were obtained by a step-scanning method: step width and fixed time were programmed for steps of 0.05° every 10 s. The X-ray diffraction photographs were taken by a flat Laue camera with a 0.5 mm diameter pinhole collimator.

## Results and Discussion

**Synthesis of Poly(propyleneimine)-Based Liquid Crystalline Dendrimers (PPILCDs).** As a relatively flexible dendritic scaffold, poly(propyleneimine) dendrimer (PPID) was selected because of well-defined and commercially available dendrimer. On the other hand, the mesogen and the length of the spacer are the primary factors determining the specific mesophases exhibited by a given side chain liquid crystalline polymer (SCLCP). A long spacer decouples the interaction between the mesogens and polymers and makes the motions of mesogens free. On the basis of these considerations, the following mesogen unit,  $\omega$ -(4'-cyanobiphenyloxy)alkyl acrylate (**1**), was synthesized from acryloyl chloride and 4'-( $\omega$ -hydroxyalkoxy)-4-biphenylcarbonitrile, which was obtained by the reaction of 4'-hydroxy-4-biphenylcarbonitrile with  $\omega$ -bromoalkane-1-ol (Scheme 1).

The Michael addition of mesogen **1** to PPIDs was carried out in THF at 50 °C for 1 week using a 1.5 molar excess amount of **1** for every primary amino end group present in the dendrimers. (Scheme 2).

The progress of reaction was monitored by TLC and <sup>1</sup>H NMR spectroscopy. The Michael addition of a primary amino group to **1** yields two adducts, such as compounds A with a secondary amino group and B with a tertiary amino group (Scheme 3).

The methylene protons (1,3) adjacent to the secondary or tertiary amine groups and the methylene protons (2,4) adjacent to ester for these adducts A and B have different chemical shifts as shown in Scheme 3. Therefore, the extent of amine alkylation by **1** was followed by the appearance of peaks 1 (2.6 ppm) and 2 (2.8 ppm) and by then the disappearance of these signals and the appearance of signals 3 (2.4 ppm) and 4 (2.7 ppm). A 1.5 molar excess amount of **1** for every primary amino end group and heating at 50 °C for 1 week were required to complete the Michael addition reaction.

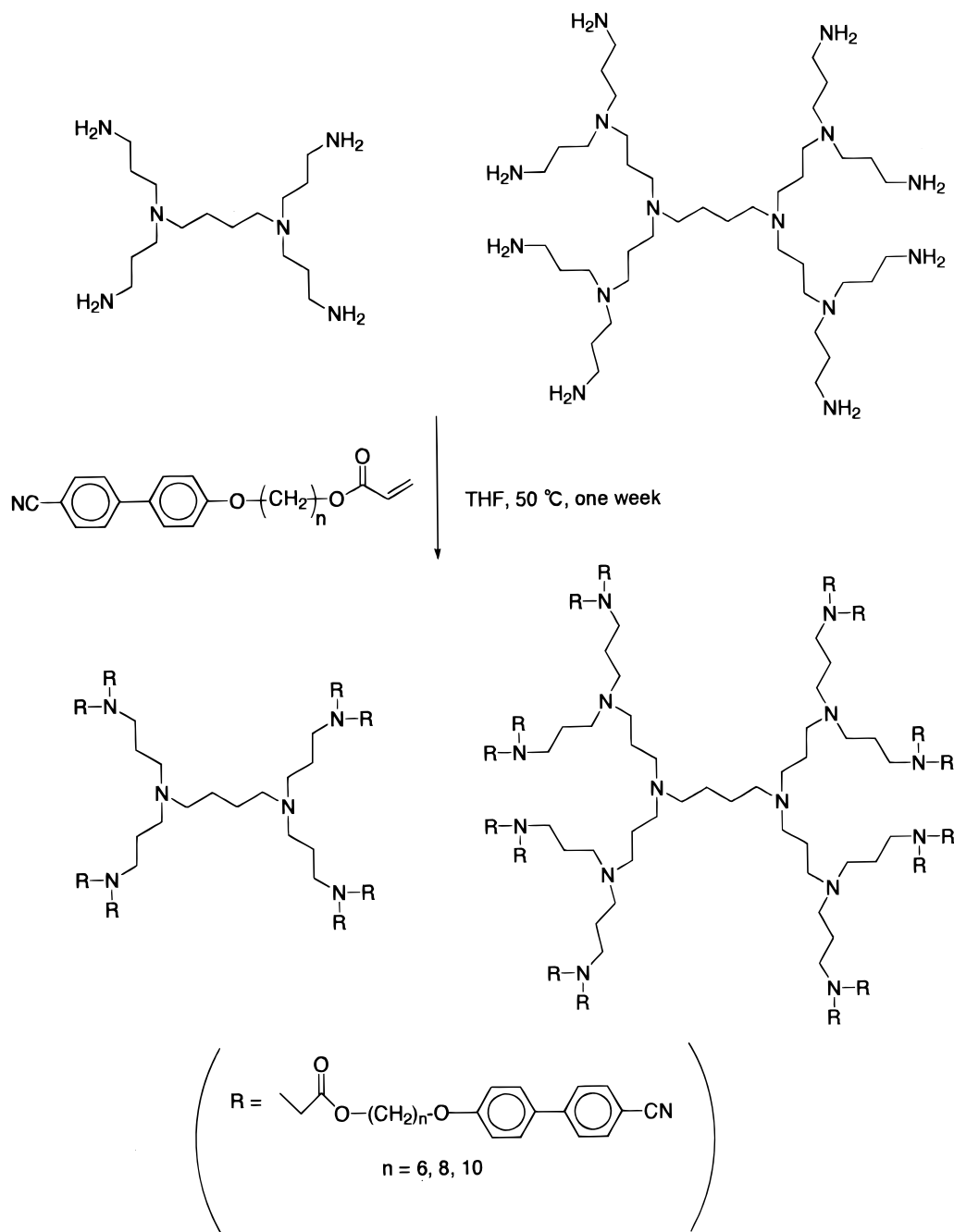
**PPILCDs** were isolated as faint yellow solids after several extractions with ethanol to remove excess amount of **1**.

**Determination of the Structure of the PPILCDs.** The IR spectra of all dendrimers showed characteristic ester carbonyl and nitrile bands at 1730 and 2230 cm<sup>-1</sup>, respectively; no peaks at 3290–3300 cm<sup>-1</sup> due to the amino groups were observed. Elemental analyses also supported the formation of the expected dendrimers.

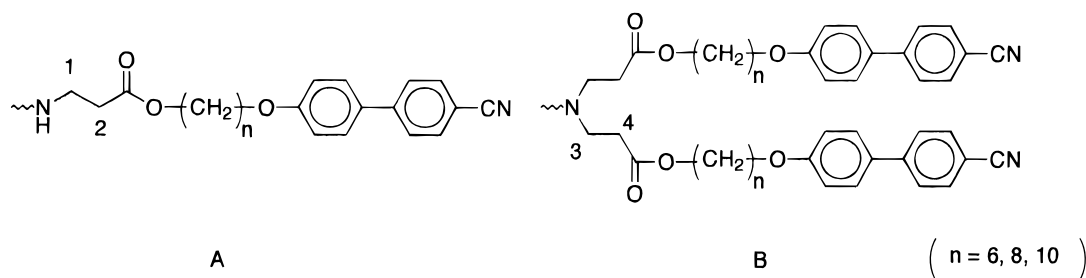
Figure 1 shows the <sup>1</sup>H NMR spectrum for **PPILCD-2-C-8**, which has 16 cyano biphenyl units at the chain ends. Some distinct features are apparent. The terminal biphenyl unit, which is para-substituted with a ether and a cyano groups, gives rise to four doublets at 6.96, 7.50, 7.61, and 7.66 ppm for the phenyl protons ortho and meta to the ether and meta and ortho to the cyano groups, respectively. The other protons in the structure were identified. All assignments are insetted in Figure 1. Other **PPILCDs** also showed similar <sup>1</sup>H NMR spectra.

The molecular weights of **PPILCDs** were determined by GPC. Figure 2 shows the typical GPC traces of **PPILCD-1-C-8** and **PPILCD-2-C-8**. Each peak is a clear unimodal molecular weight distribution. A shift toward lower elution time and higher molecular weights are obtained on going from **PPILCD-1-C-8** to **PPILCD-2-C-8**. The relative  $M_n$  and  $M_w$  values of PPILCDs for standard polystyrene are summarized in Table 1. Poly-

Scheme 2



Scheme 3



dispersity also suggests that PPILCDs have a very narrow molecular weight distributions.

The most conclusive molecular weights of dendrimers were determined by MALDI-TOF mass spectrometry. The MALDI-TOF mass spectrum of **PPILCD-2-C-6** shows one signal that is clearly due to the formation of

the desired dendrimers with 16 mesogens (Figure 3). The  $m/z$  value of the signal ( $6389.4 - 22.9 = 6366.5$ ) corresponds to the calculated value of  $m/z = 6364.2$ . The results are also listed in Table 1. The molecular ion peaks containing  $\text{Na}^+$  ions or protons for the dendrimers were consistent with those expected for the **PPILCDs**.



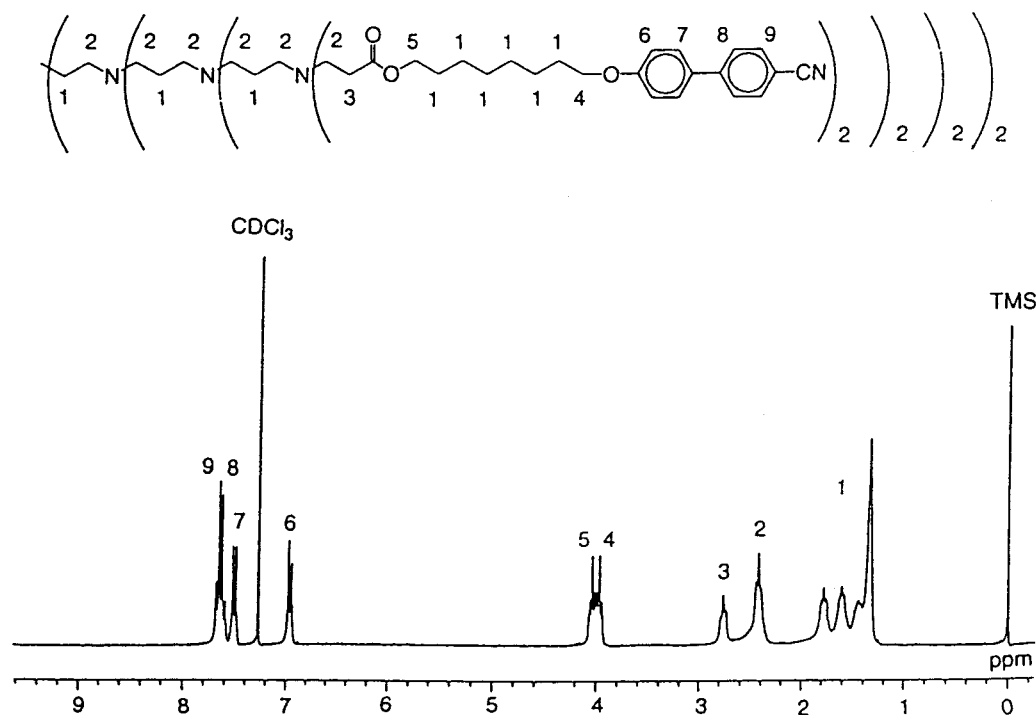


Figure 1.  $^1\text{H}$  NMR spectrum of PPILCD-2-C-8 in  $\text{CDCl}_3$ .

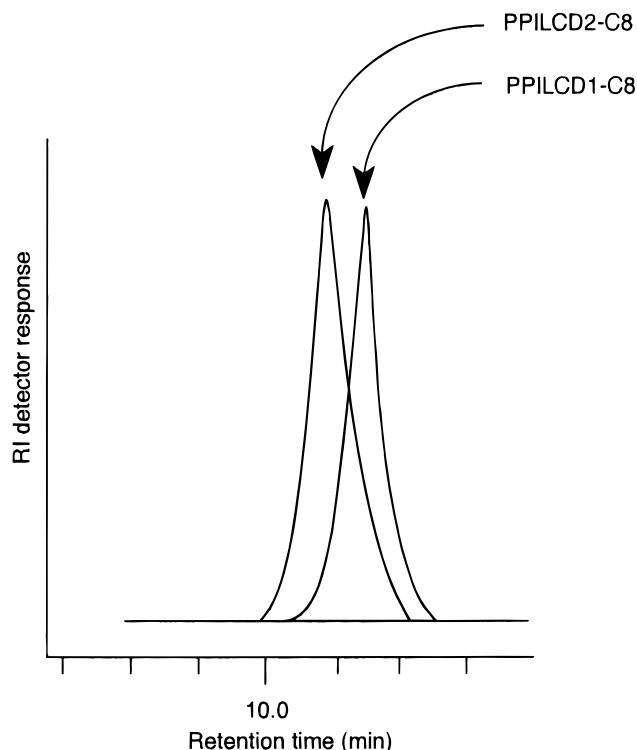


Figure 2. GPC traces of PPILCD-1-C-9 and PPILCD-2-C-8 in THF at  $40^\circ\text{C}$ .

These results clearly indicate the formation of the desired PPILCDs.

**Phase Transitions and Structures of PPILCDs.** The DSC traces of PPILCD-1s and PPILCD-2s for the second-heating/cooling processes are illustrated in Figures 4 and 5, respectively. They exhibited a glass transition ( $T_g$ ) and a distinct endothermic peak on the heating DSC curves. The  $T_g$  values of PPILCDs remained almost unchanged despite different lengths of the flexible spacers connecting the dendritic scaffolds

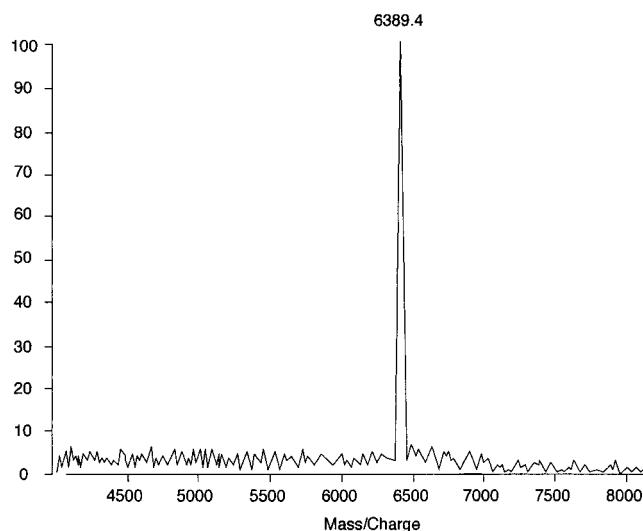


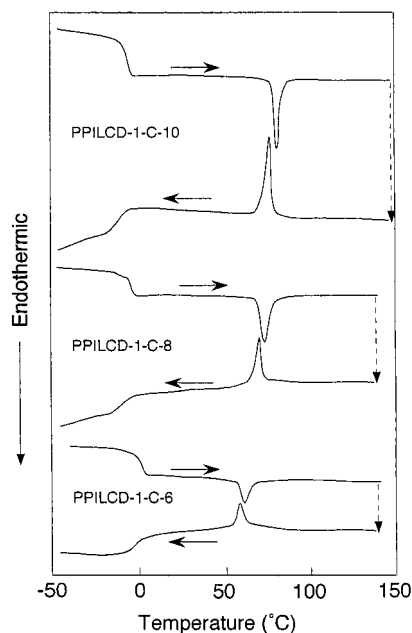
Figure 3. MALDI-TOF mass spectrum of PPILCD-2-C-6. The spectrum was measured using 2,5-dihydroxybenzoic acid as the matrix.

Table 1. Molecular Weights and Distributions of PPILCDs

| dendrimer    | $M(\text{calcd})$ | $M(\text{exptl})$ | $M_n$   | $M_w/M_n$ |
|--------------|-------------------|-------------------|---------|-----------|
| PPILCD-1-C6  | 3111.99           | 3111.2            | 8162.08 | 1.05      |
| PPILCD-2-C6  | 6364.23           | 6366.4            | 10659.7 | 1.06      |
| PPILCD-1-C8  | 3336.43           | 3336.0            | 8072.94 | 1.06      |
| PPILCD-2-C8  | 6780.83           | 6780.6            | 10146.5 | 1.07      |
| PPILCD-1-C10 | 3558.17           | 3562.3            | 7840.02 | 1.05      |
| PPILCD-2-C10 | 7261.95           | 7267.5            | 10406.4 | 1.09      |

with the mesogens. Moreover, they did not depend on the generation of the dendritic cores. The  $T_g$ s of PPILCDs are about 35 K lower than those of poly(propyleneimine)-based LCDs coupled with rigid mesogens by amide linkages which induce the intermolecular hydrogen bonds between amide groups.<sup>14</sup>

The focal-conic fan textures corresponding to smectic liquid crystalline phase were observed at room temper-



**Figure 4.** DSC thermograms of 2nd-heating and cooling processes for **PPILCD-1s**. Heating and cooling rates are  $10\text{ }^{\circ}\text{C min}^{-1}$ .

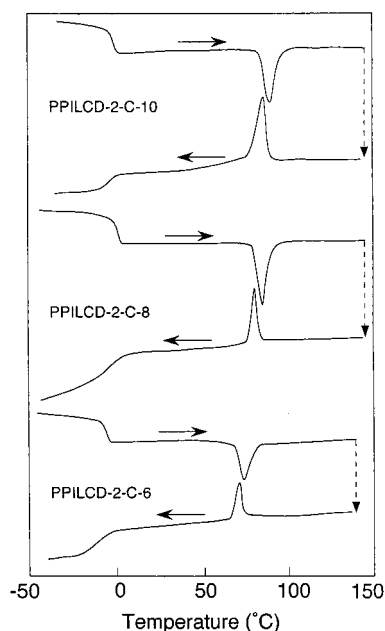


**Figure 5.** DSC thermograms of 2nd-heating and cooling processes for **PPILCD-2s**. Heating and cooling rates are  $10\text{ }^{\circ}\text{C min}^{-1}$ .

ature under the POM, as shown in Figure 6. **PPILCDs** exhibited a thermotropic liquid crystalline nature, due to comparatively flexible dendritic scaffolds and ester linkages. The smectic textures disappeared above the temperatures of the endothermic peaks on the DSC curves and changed into the dark field under the POM with crossed polarizers. Thus, the endothermic peaks are due to smectic/isotropic phase transition. The wide-angle X-ray scattering (WAXS) patterns of **PPILCDs** were measured at room temperature to determine the structure of the smectic phase. The WAXS photographs showed Debye–Sherrer rings at the small angle area and a diffuse halo at the wide angle area. Accordingly the smectic liquid crystalline phases were assigned to smectic A ( $S_A$ ). The diffuse reflection at the wide angle

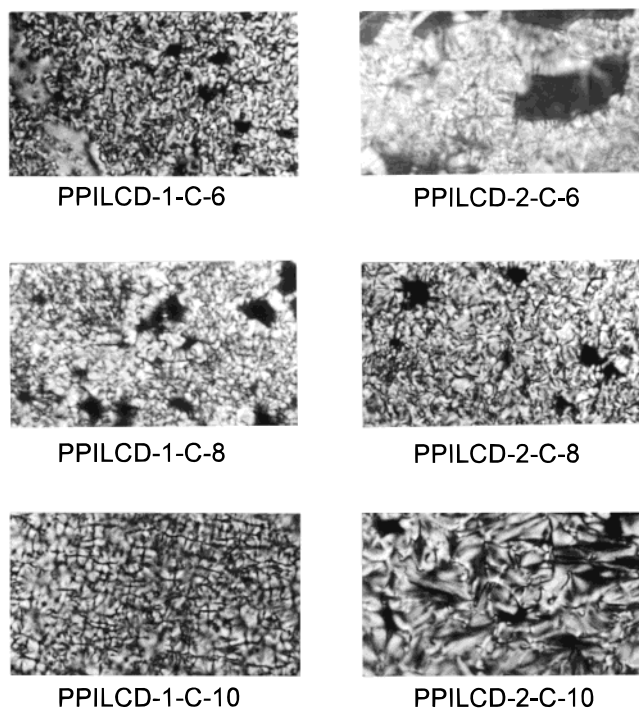


**Figure 6.** Polarizing optical micrographs of **PPILCDs** taken at room temperatures.

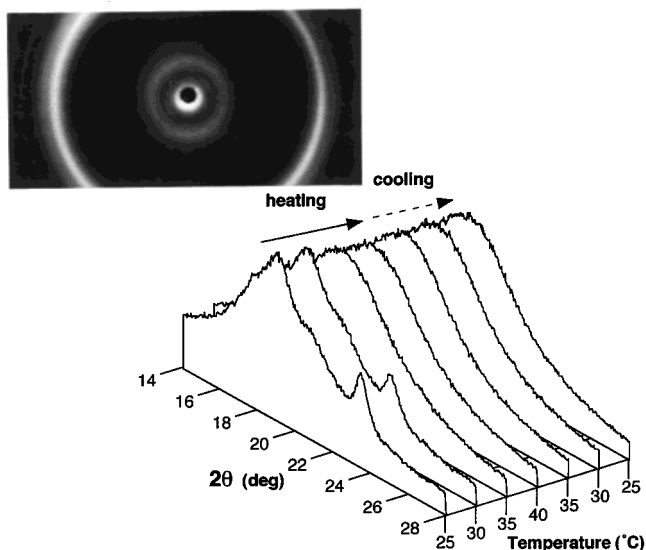


**Figure 7.** Change in WAXS profiles of **PPILCD-2-C-10** during heating and cooling processes. X-ray photograph of as-synthesized sample was taken at  $25\text{ }^{\circ}\text{C}$ .

area was observed at approximately  $0.45\text{ nm}$ , which corresponds to the lateral distance between the mesogens. These results were analogous to those reported by Baars et al.<sup>16</sup>

In the case of **PPILCD-2-C-10** with long flexible spacers, the as-made sample, however, exhibited several sharp rings in the wide angle area, as shown in Figure 7 (X-ray photograph). It suggests that a highly ordered smectic phase formed in the sample during the synthetic process. If a hexatic phase is formed in the sample, the  $d$  spacings ( $d_{hkl}$ ) of the X-ray reflections observed at the wide-angle area exhibit the relationship of the hexagonal packing mode;  $d_{110}:d_{110}:d_{210} = 1:1/\sqrt{3}:1/\sqrt{7}$ . But, their  $d$  spacings obtained did not show the above relationship; the smectic phases were not assigned to hexatic smectic B. Thus, it might be a highly ordered

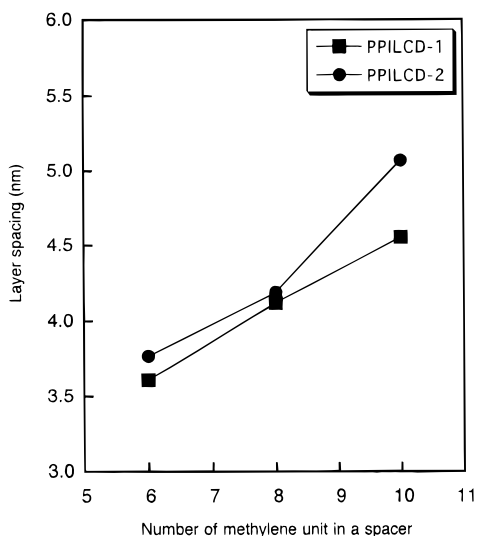


**Figure 8.** Changes in layer spacing of smectic A for **PPILCDs** against the number of methylene units in a flexible spacer.

smectic phaselike smectic E ( $S_E$ ). However, the  $S_E$ -like phase disappeared once the sample was annealed above 35 °C. The change in the WAXS patterns during heating and cooling processes is shown in Figure 7. The WAXS trace measured at 25 °C indicates some reflections at  $2\theta = 18, 20$ , and 23°. They disappeared at 35 °C, and only diffuse scattering remained. The reflections at the small angle area, corresponding to a smectic layer structure, were observed above 30 °C. This is evidence that the  $S_E/S_A$  phase transition occurred at 30 °C. The phase transition did not occur down to room temperature. The  $S_E$ -like structure was formed only in the as-made sample of **PPILCD-2-C-10**. This can be explained as follows: The dendritic cores were stressed by the formation of comparatively highly ordered smectic structure like  $S_E$  on the purification and precipitation process. The core chains might be relaxed by annealing, and the above highly ordered smectic structure could not be formed in the system on cooling. It may be possible to observe the  $S_E$  phase if the length of the flexible spacer is increased to decouple the mobility of the mesogens from the dendritic core.

Figure 8 indicates the changes in layer spacings of  $S_A$  for **PPILCDs** against the number of methylene unit in a spacer. As the layer spacing increased with increasing the number of methylene units, the chains of flexible spacers may be extended. If we suppose that the chains in the dendritic cores are extended, the mesogens can be overlapped in the smectic layers as shown in Figure 9. The molecular model of **PPILCD 10** was built up using Cerius 2. The mesogens in a dendritic core were constructed in parallel when the starting model was built, and then the molecular model was minimized using the force field "pcff300". In Figure 9, the three molecules minimized were placed to construct a smectic layer structure having a layer spacing of 4.5 nm, which was estimated from the X-ray diffraction experiment.

The changes in the  $S_A$ /isotropic phase transition temperatures ( $T_i$ ) were illustrated in Figures 10 and 11, which were estimated on the second heating DSC traces (Figures 4 and 5).  $T_i$  values linearly increased with increasing the number of methylene unit in a flexible spacer; the temperature range of  $S_A$  phase expanded. These behaviors are due to decoupling of the mobility of the terminal mesogens from that of the dendritic core.

This decoupling is similar to that of conventional SCLCPs.

Note that the temperatures of endothermic and exothermic peaks are very close each other; the supercooling at the isotropic/smectic phase transition of **PPILCDs** is very small, which was only 3 K. Generally, SCLCPs exhibit comparatively large supercooling due to the restriction of the main chain. These very low degrees of supercooling **PPILCDs** results from the unique structure of the dendrimer. In the isotropic phase, if the chains in a dendritic core are relaxed with increasing temperature and the core spreads out, the terminal mesogens fluctuate and the isotropic state will be obtained. In the isotropic state, there might be few entanglements between dendrimers because of the effect of molecular structure of the dendrimers. Thus, it is easy to re-form the smectic structure on cooling from the melt state.

**Smectic Structures of PPILCD-2-C-10** Figure 12 shows the optical textures of **PPILCD-2-C-10** cooled at various cooling rates from the isotropic melt. The cooling rates had no influence on their fan textures. However, dark field regions were observed in some places in the smectic texture when cooling slowly. The dark fields expanded greatly when cooling took place at 0.5 °C min<sup>-1</sup>.

The changes in optical textures of **PPILCD-2-C-10** during cooling at 0.5 °C min<sup>-1</sup> were shown in Figure 13. The batonnet textures occurred in the isotropic matrix, and they incorporated and changed to the fan textures. In further cooling, the fan textures started disappearing at 89 °C, and the dark field expanded gradually with cooling. The structural change stopped at approximately 82 °C, and the fan texture and the dark field also coexisted at the room temperature.

A typical conoscopic pattern was observed at the dark field area, as shown in Figure 14. It suggests that homeotropic orientation structures were formed in the sample, while the surface of the glass substrate was not treated to bring about a homeotropic orientation for the mesogens. We followed up the arrangement of the mesogen in the film as follows:

In general, the homeotropic orientation of the mesogens exhibits a dark field under the POM with crossed polarizers, because of the optical isotropy on the through view as illustrated in Figure 15a in which the mesogens are upright on the film surface. If the sample film is tilted up in the direction of the thick arrow as shown in Figure 15b, it is expected to exhibit optical anisotropy on the through view, as the mesogens are also tilted. Tilting the sample seems to increase the reflective index in the direction of the arrow and gives an optical anisotropy on the through view, since the cyanobiphenyl mesogen has a high anisotropy of dielectric constant in the direction of its molecular axis. Thus, the tilted sample is expected to exhibit birefringent light and an optically positive nature in the direction of the thick arrow.

Birefringent light was observed under the crossed polarizers, when the **PPILCD-2-C-10** film was tilted up in the direction of the thick arrow, as shown in Figure 16. The tilt angle was about 15°. The retardation of the sample film was observed under the POM with crossed polarizers using a sensitive color plate ( $\lambda = 530$  nm) to examine the alignment of the mesogens. The optical micrographs of the tilted film were shown in Figure 16, indicating three geometrical arrangements

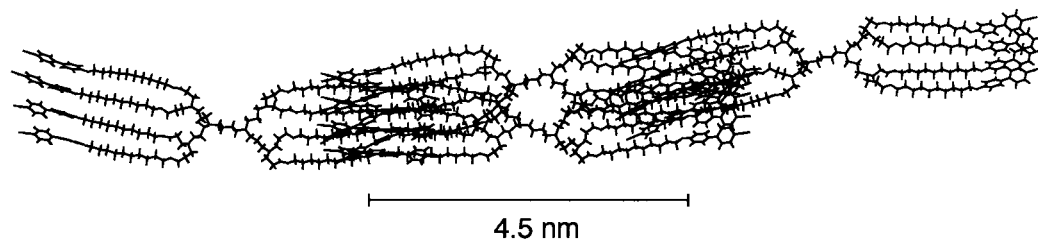


**Figure 9.** Structural representation of the  $S_A$  phase for **PPILCD-1-C10** built by using Cerius<sup>2</sup>.

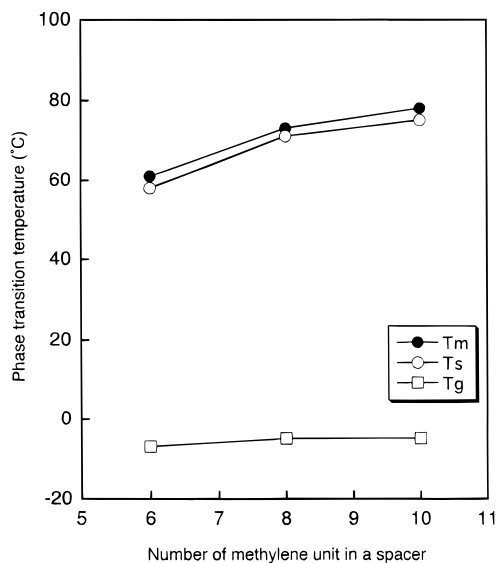


**Figure 10.** Changes in phase transition temperatures of **PPILCD-1s** plotted against the number of methylene units in a flexible spacer of **PPILCD-1s**. Key:  $T_m$ , smectic/isotropic phase transition;  $T_s$ , isotropic/smectic phase transition;  $T_g$ , glass transition.

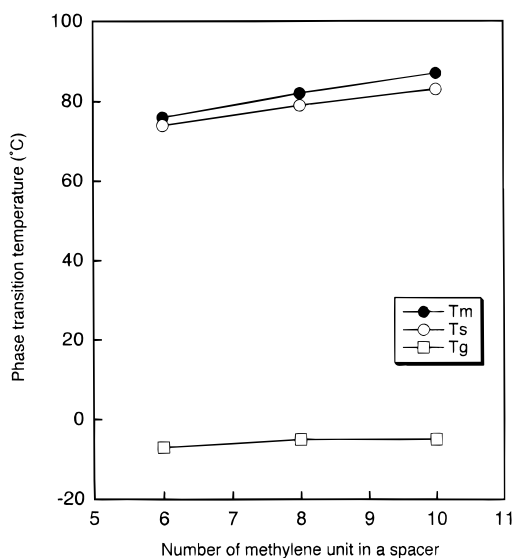


**Figure 11.** Changes in phase transition temperatures of **PPILCD-2s** plotted against number of methylene unit in a flexible spacer of **PPILCD-2s**. Key:  $T_m$ , smectic/isotropic phase transition;  $T_s$ , isotropic/smectic phase transition;  $T_g$ , glass transition.

for the film, polarizers, and sensitive color plate. The tilted film exhibited a blue color at the geometrical arrangement (1) where the film was put at diagonal position to the polarizers and was parallel to the optical axis ( $z'$  axis) of the sensitive color plate. It turned purple at the arrangement (2) which was the position of

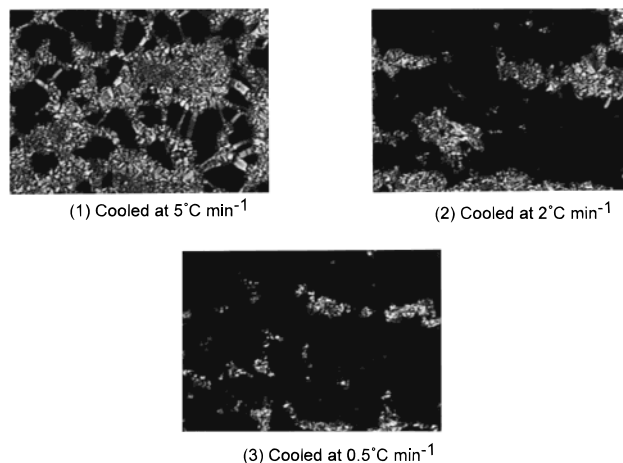


**Figure 12.** Polarizing optical textures of **PPILCD-2-C-10** cooled at various rates from the melt.

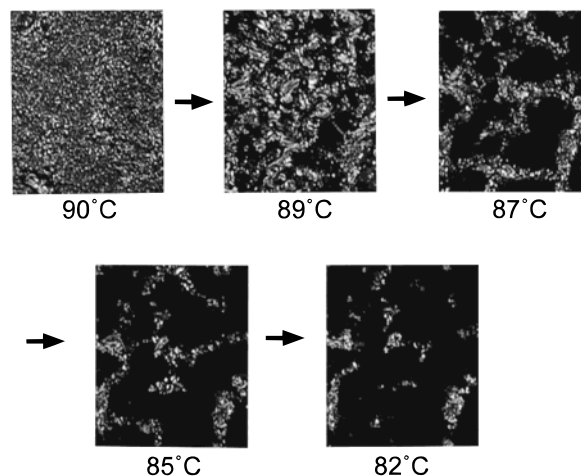


**Figure 13.** Polarizing optical micrographs of **PPILCD-2-C-10** during cooling at  $0.5\text{ }^{\circ}\text{C min}^{-1}$ .

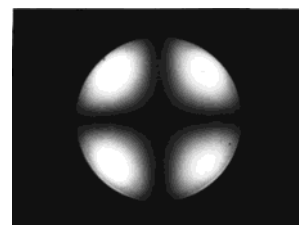


**Figure 14.** Conoscopic pattern observed at the dark field of Figure 12 (photograph 3).

extinction. And, at the arrangement (3) where the sample was put at diagonal position to the polarizers and was vertical to the  $z'$  axis of the sensitive color plate, it turned yellow. Consequently, the tilted sample indicated an optically positive nature in the direction of the thick arrow; that is, the reflective index in this direction became higher than that in the direction vertical to the



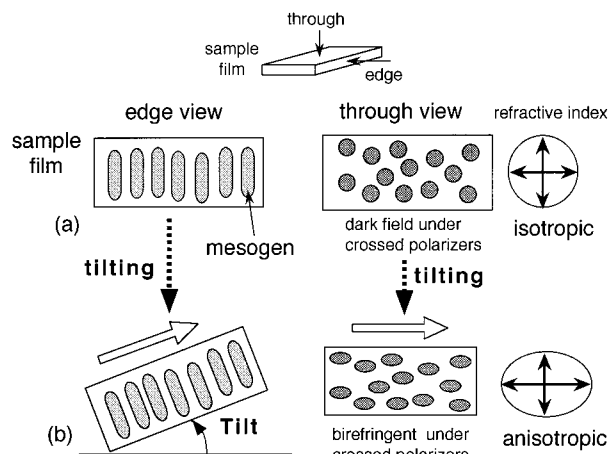


**Figure 15.** Schematic representations for homeotropic orientation and optical property. (a) Homeotropic orientation of mesogens is observed: the mesogens are upright on the film surface; the through view of the film exhibits an optically isotropic nature. (b) The film is tilted; optical anisotropy is observed on the through view.

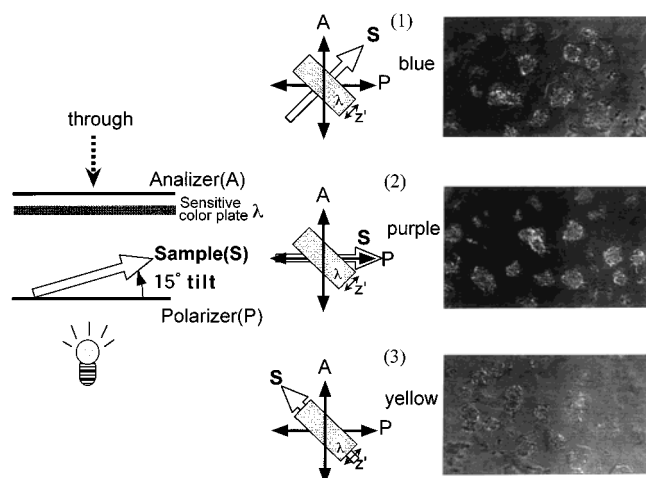


**Figure 16.** Polarizing optical micrographs observed with closed polarizers and sensitive color plate ( $\lambda = 530$  nm), and geometrical arrangement of sample, polarizers, and sensitive color plate. The thick arrow denotes the same film tilted up in the direction of the arrow.

arrow. This finding indicates that the mesogens are upright on the film surface.

As described above, it was confirmed that homeotropic orientation of the mesogens was allowed to take place in **PPILCD-2-C-10**. However, it is hard to explain the reason the homeotropic structure was generated during the slow cooling process. In general, the formation of a homeotropic structure depends on the surface of the substrate. In this case, as the surface of the glass substrate was not treated to bring about a homeotropic orientation for the mesogens, it might be ascribed to the three-dimensional structures of the dendrimers built on the surface of the glass plate. If the mesogens of **PPILCD-2-C-10** stand out on the surface of the glass substrate, it is possible that the mesogens rearrange and assemble to the homeotropic structure on cooling. It is necessary to analyze the steric structures of **PPILCD-2-C-10** on the glass plate. Coen et al. suggested that mesogens of carbosilane dendrimers might be oriented perpendicular to a mica surface.<sup>15</sup>

Meijer et al. also reported that poly(propyleneimine) dendrimers with cyanobiphenyl mesogens oriented into

an antiparallel arrangement, yielding an interdigitated bilayer even in the higher generation LCDs.<sup>16</sup> Moreover, in the case of amphiphilic dendrimers,<sup>17</sup> stable monolayers formed at the air–water interface. It has been suggested that the amphiphilic chains were aligned perpendicular to the water surface and the dendritic surfactants adopt a cylindrical shape at the interface.<sup>17</sup> Thus, the liquid crystalline dendrimers and amphiphilic dendrimers exhibit self-assembly. It is possible that the PPILCDs form the homeotropic structure on the glass substrate in which the terminal mesogens are aligned perpendicular to the glass surface.

## Conclusions

Our studies indicate that **PPILCDs** with a relatively flexible dendritic scaffold were successfully synthesized from poly(propyleneimine) dendrimers and  $\omega$ -(4'-cyano-biphenyloxy)alkyl acrylate (**1**). **PPILCDs** showed smectic liquid crystalline natures and very low degrees of supercooling. Furthermore, the homeotropic orientation was observed in **PPILCD-2-C-10** on the glass plate. **PPILCDs** also exhibit self-assembly. The interaction between **PPILCDs** and the glass plate and the formation of homeotropic structures are under investigation. These properties of **PPILCDs** are of interest in the fields of high-speed switching devices and alignment of liquid crystals for liquid crystal devices.

**Acknowledgment.** We indebted to Sadao Kato for the technical assistance and Takeyoshi Takahashi for performing the elemental analyses.

## References and Notes

- (1) Tomalia, D. A.; Naylor, A. M.; Goddard, W. A. *Angew Chem. Int. Ed. Engl.* **1990**, *29*, 138.
- (2) Frechet, J. M. *Science* **1994**, *263*, 1710.
- (3) de Brabander-van den Berg, E. M. M.; Meijer, E. W. *Angew. Chem., Int. Ed. Engl.* **1993**, *32*, 1308.
- (4) Zeng, F.; Zimmerman, S. C. *Chem. Rev.* **1997**, *97*, 1681.
- (5) Matthews, O. A.; Shipwa, A. N.; Stoddart, J. F. *Prog. Polym. Sci.* **1998**, *23*, 1.
- (6) Stevelmans, S.; van Hest, J. C. M.; Jansen, J. F. G. A.; van Bortel, D. A. F. J.; de Brabander-van den Berg, E. M. M.; Meijer, E. W. *J. Am. Chem. Soc.* **1996**, *118*, 7398.
- (7) Hawker, C. J.; Wooley, K. L.; Frechet, J. M. J.; *J. Chem. Soc., Perkin Trans. 1* **1993**, *21*, 1287.
- (8) Sayed-Sweet, Y.; Hedstrand, D. M.; Spinder, R.; Tomalia, D. A. *J. Mater. Chem.* **1997**, *7*, 1199.
- (9) Percec, V.; Chu, P.; Ungar, G.; Zhou, J. *J. Am. Chem. Soc.* **1995**, *117*, 11441.
- (10) Ponomarenko, S. A.; Rebrov, E. A.; Bobrovsky, A. Y.; Boiko, N. I.; Muzafarov, A. M.; Shibaev, P. *Liq. Cryst.* **1996**, *21*, 1.
- (11) Lorenz, K.; Holter, D.; Stuhn, B.; Mulhaupt, R.; Frey, H. A. *Adv. Mater.* **1996**, *8*, 414.
- (12) Busson, P.; Ihre, H.; Hult, A. *J. Am. Chem. Soc.* **1998**, *120*, 9070.
- (13) Suzuki, K.; Haba, O.; Nagahata, R.; Yonetake, K.; Ueda, M. *High Perform. Polym.* **1998**, *10*, 231.
- (14) Yonetake, K.; Morishita, T.; Suzuki, K.; Nagahata, R.; Ueda, M. *High Perform. Polym.* **1998**, *10*, 373.
- (15) Coen, M. C.; Lorenz, K.; Kressler, J.; Frey, H.; Mulhaupt, R. *Macromolecules* **1996**, *29*, 8069.
- (16) Baars, M. W. P. L.; Sontjents, S. H. M.; Fisher, H. M.; Peerlings, H. W. I.; Meijer, E. W. *Chem.-Eur. J.* **1998**, *4*, 2456.
- (17) Schenning, A. P. H. J.; Elissen-Roman, C.; Weener, J.-W.; Baars, M. W. P. L.; van der Gaast, S. J.; Meijer, E. W. *J. Am. Chem. Soc.* **1998**, *120*, 8199.